BPB Reports

Regular Article

Removal of Methylene Blue from Aqueous Media Using Coffee Inner Husks

Fumihiko Ogata,[a] Yugo Uematsu,[a] Noriaki Nagai,[a] Yuuya Hashimoto,[a] Chalermpong Saenjum,[b,c] Shigeharu Tanei,[d] and Naohito Kawasaki[a,e,*]

[a]*Faculty of Pharmacy, Kindai University, 3-4-1 Kowakae, Higashi-Osaka, Osaka 577-8502, Japan;* [b]*Faculty of Pharmacy, Chiang Mai University, Suthep Road, Muang District, Chiang Mai, 50200, Thailand;* [c]*Center of Excellence for Innovation in Analytical Science and Technology for Biodiversity-based Economic and Society (I-ANALY-S-T_B.BES-CMU), Chiang Mai University, Chiang Mai, 50200, Thailand;* [d]*Faculty of Pharmaceutical Sciences, Nihon Pharmaceutical University, 10281 Komuro, Ina-machi, Kitaadachi-gun, Saitama, 362-0806, Japan;* [e]*Antiaging Center, Kindai University, 3-4-1 Kowakae, Higashi-Osaka, Osaka 577-8502, Japan*

Received June 10, 2025; Accepted June 23, 2025

Virgin coffee inner husk (VCIH) and VCIH calcined at 1000°C (CIH1000) were prepared in this study. These adsorbents were characterized by scanning electron microscopy imaging, thermal analysis, specific surface area measurements, surface functional groups, and point-of-zero charge (pH_{pzc}). The adsorption capacity of methylene blue (MB) was greater for CIH1000 than for VCIH. In addition, the MB adsorption capacity was evaluated by demonstrating the effect of initial concentration, temperature, contact time, and pH on the adsorption. The results were fitted to both the Langmuir model (correlation coefficient: 0.915–0.997) and the pseudo-second-order model (correlation coefficient: 0.989–0.997). To elucidate the MB adsorption mechanism, elemental distributions and binding energies were characterized and the components of MB (carbon, sulfur, and nitrogen) were detected after adsorption. These findings provide useful information for the removal of MB from aqueous media.

Key words coffee inner husk, methylene blue, adsorption, calcination

INTRODUCTION

Effluents containing very small amounts of dye can cause serious negative impacts on the environment and ecosystem by limiting light penetration, leading to a decrease in photosynthesis of aquatic species, among other adverse effects.[1,2] In addition, an estimated 7 × 10^5 tons of different coloring chemicals from approximately 1.0 × 10^5 commercially available dyes are produced each year.[3,4] Methylene blue (MB) is an essential organic dye broadly used in various fields such as biology, chemistry, and the medical and dyeing industries.[5,6] Because of its aromatic ring, MB is particularly toxic and arduous and causes symptoms such as vomiting, nausea, anemia, and hypertension in humans with long-term exposure.[7-9] Therefore, the development of general methods of treating wastewater that contains dyes, particularly MB, has attracted much attention globally.[10]

Various physicochemical and/or biological processes such as chemical precipitation, coagulation, reverse osmosis, adsorption, advanced oxidation processes, and aerobic and/or anaerobic microbial degradation are generally used to treat MB-contaminated wastewater.[11] Among the existing methods, adsorption is a promising process in waste and/or wastewater treatments. It also has low initial costs, produces few secondary pollutants, and is relatively simple in terms of the design and operation of the treatment equipment. In addition, a wide variety of adsorbents are available, which makes the process cost-effective and enables the removal of various groups of pollutants.[10]

Coffee inner husk is major waste generated from coffee processing in industry, and the conversion of waste biomass into adsorbents can reduce the amount of disposed material and environmental pollution.[12] In addition, to increase the efficiency of bioadsorbents in the adsorption of dyes from aqueous media, various chemical modifications such as acid and/or thermal treatments have been used to improve the ability of adsorbents to adsorb of dyes.[13] In particular, simple traditional pyrolysis treatments can change properties such as the number of functional groups, resulting in a hard support with a greater surface area.[14]

The present study is aimed at exploring the effects of pyrolysis treatments on coffee inner husk. The prepared adsorbent was used to remove MB from aqueous media, and the effect of the initial concentration, temperature, contact time, and pH was studied. A detailed analysis of the adsorption data was conducted using equilibrium and kinetic models. We expect

---

*To whom correspondence should be addressed. e-mail: kawasaki@phar.kindai.ac.jp

our results to contribute to the sustainable development of coffee inner husk as waste biomass and to evaluations of its suitability as an adsorbent for purifying wastewater containing MB.

MATERIALS AND METHODS

Materials Methylene blue (MB, $C_{16}H_{18}N_3SCl \cdot 3H_2O$, CAS RN: 7220-79-3) was obtained from FUJIFILM Wako Pure Chemical (Japan). Virgin coffee inner husk (VCIH) was purchased from Chiang Mai in Thailand. The calcination procedure was conducted at 1000°C for 2 h in a muffle furnace; the resultant product is referred to as CIH1000.

Characterization of Prepared Adsorbents The morphology of the prepared adsorbents was characterized by low-vacuum-pressure scanning electron microscopy (SU1510, Hitachi High-Technologies, Tokyo, Japan). Thermogravimetry–differential thermal analysis (TG–DTA) was conducted using a TG8210 thermogravimetric analyzer (Rigaku, Japan), and specific surface area was analyzed using a BELSORP MINI X pore-size distribution analyzer (MicrotracBEL, Japan). Surface functional groups were characterized, and the point of zero charge (pH_{pzc}) was measured using previously reported methods.[15,16]

MB Adsorption Capacity of VCIH and CIH1000 Batch adsorption experiments were conducted, and various parameters, including the initial MB concentration (10–1000 mg/L), adsorption temperature (7, 25, and 45°C), contact time (0.5–24 h), and solution pH (2, 4, 6, 8, and 10), were varied. Each experiment involved adding precisely weighed adsorbent (0.05 g) to 50 mL of MB solution and reacting the resultant mixture for 24 h under constant agitation at 100 rpm. After the reaction, the sample solution was filtrated through a 0.45-µm membrane filter. The initial and/or equilibrium MB concentration was determined from the absorbance measured at a wavelength of 664 nm using a UV–visible spectrophotometer (UV-1280, Shimadzu, Kyoto, Japan). The amount of MB adsorbed was calculated using the initial and equilibrium concentrations. The calibration curve range was confirmed in the preliminary experiments. All data are expressed as mean ± standard deviation.

Finally, to elucidate the mechanism of MB adsorption onto the prepared adsorbents, binding energy measurements were conducted and the elemental distribution was characterized before and after adsorption using an Axis-Nova spectrometer (Shimadzu, Kyoto, Japan) and a field-emission electron-probe microanalyzer (JXA-8530F, JEOL, Tokyo, Japan), respectively.

RESULT AND DISCUSSION

Properties of VCIH and CIH1000 Figure 1 shows SEM images of VCIH and CIH1000, along with their thermal analysis results. The coffee inner husk surface was broken by calcination. In addition, the TG trace shows a slight decrease in mass at ~100°C because of the evaporation of water on the adsorbent's surface. Moreover, the mass clearly decreased in the temperature range 300–500°C because of combustion. In a previous study, the calcination of waste biomass at 300–600°C was reported to strongly affect the surface functional groups; in particular, surface functional groups such as carboxylic, phenolic, and other groups disappeared at these calcination temperatures.[17]

The physicochemical characteristics of VCIH and CIH1000 are shown in Table 1. The specific surface area of CIH1000 was greater than that of VCIH (not detected). The pH_{pzc} value of CIH1000 and VCIH was 4.62 and 7.12, respectively. The calcination of VCIH strongly affected its surface functional groups, indicating a decrease in the amount of acidic functional groups and a slight increase in the amount of basic functional groups. Similar trends were observed in a previous study.[17]

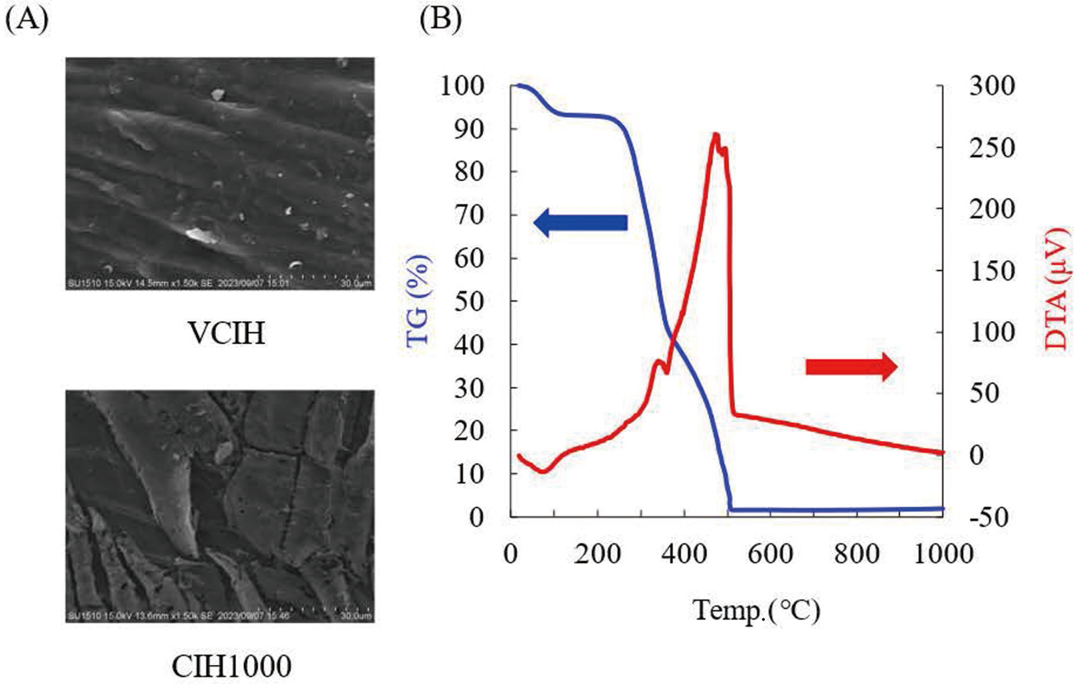

Fig. 1. SEM Images (A) and Thermal Analysis (B) of Adsorbents

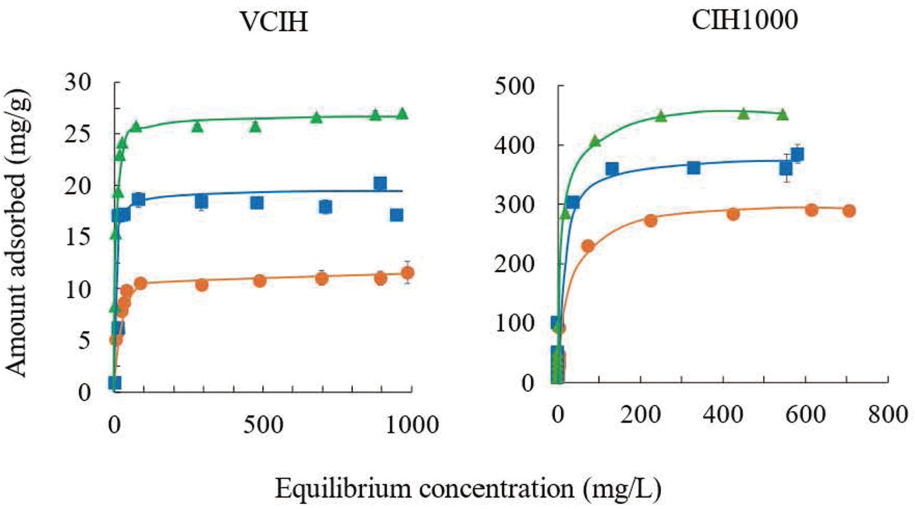

Fig. 2. Adsorption Isotherms of MB onto VCIH and CIH1000

Initial concentration: 10–1000 mg/L, sample volume: 50 mL, adsorbent: 0.05 g, temperature: 7, 25, and 45°C, contact time: 24 h, 100 rpm, ●: 7°C,■: 25°C,▲: 45°C

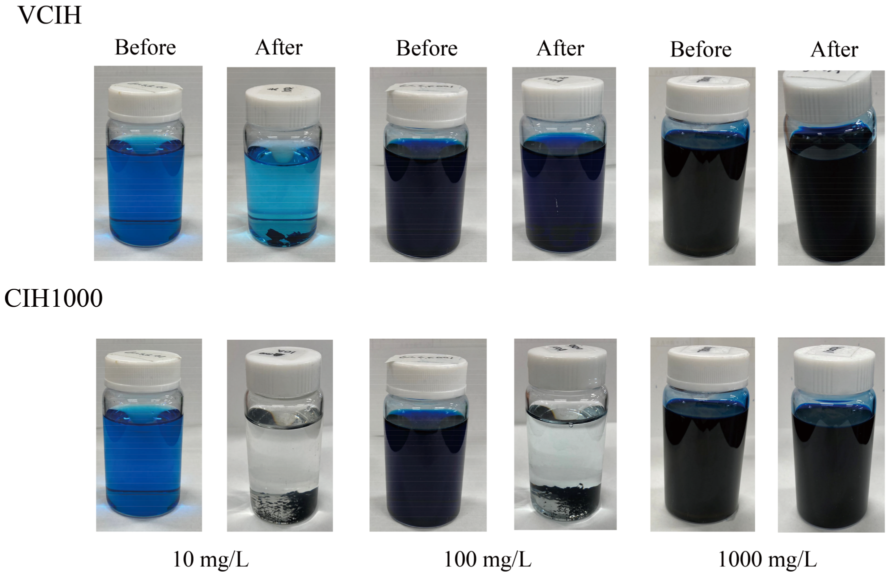

Fig. 3. Sample Solution before and after Adsorption

Table 1. Physicochemical Characteristics of Adsorbents

Samples	Specific surface area (m^2/g)	pH_{pzc}	Acidic functional groups (mmol/g)	Basic functional groups (mmol/g)
VCIH	N.D.	4.26	2.31	4.45
CIH1000	953	7.12	1.37	4.80

Adsorption Isotherms of MB onto VCIH and CIH Adsorption isotherms of MB onto VCIH and CIH1000 are shown in Fig. 2. In addition, a sample solution before and after adsorption is shown in Fig. 3. The MB adsorption ability of VCIH and CIH1000 increased with increasing adsorption temperature. Adsorption processes are generally classified as either exothermic or endothermic. The increase in adsorption ability with increasing temperature indicates that the adsorption capacity of the adsorbents may have increased or decreased with increasing temperature. An increase in the adsorption capacity with increasing temperature indicates an endothermic adsorption process.18) In addition, adsorption temperature plays an important role in controlling the strength of the adsorptive forces between the adsorbent and adsorbate molecules.19) Therefore, the process of MB adsorption onto VCIH and CIH1000 is endothermic, where the MB molecules need energy to move around and penetrate deeper into the pores of VCIH and CIH1000 at higher temperatures.18)

The two fundamental isotherms used to elucidate the adsorption characteristics of VCIH or CIH1000 and to evaluate the adsorption equilibrium for the removal of MB are the Langmuir model and the Freundlich model.20,21)

The Langmuir model is given as

$$1/q = 1/(W_s \alpha C_e) + 1/W_s, \quad (1)$$

where q represents the amount of MB adsorbed (mg/g), W_s represents the maximal monolayer adsorption capacity of MB (mg/g), C_e represents the equilibrium concentration of MB (mg/L), and α denotes the Langmuir constant (binding energy) (L/mg).

The Freundlich model is given as

$$\log q = \frac{1}{n}\log C_e + \log k, \quad (2)$$

where the value of n is used to evaluate the adsorption nature, whereas k denotes the Freundlich constant. Three outcomes for n are demonstrated: $n > 1$ (chemical); $n = 1$ (linear operation); and $n < 1$ (physical) (Table 2).

The results in Table 2 show that the value of the linear correlation coefficient (r) in the Freundlich isotherm model is relatively low (VCIH: 0.803–0.895, CIH1000: 0.944–0.963), indicating its unsuitability for describing the adsorption of MB onto the VCIH and CIH1000. Conversely, its value is high in the Langmuir isothermal model (VCIH: 0.921–0.997, CIH1000: 0.915–0.990, except for 45°C in CIH1000), suggesting that this model can be used to characterize the equilibrium adsorption. In addition, according to the Langmuir model, the maximum adsorption capacity (W_s) of MB is close to the value of (q) in the experimental data.[22] Similar trends have been observed in previous studies.[23,24] Our results show that the adsorption of MB is a dynamic chemisorption process based on the adsorption affinity in terms of surface functional groups and bonding energy.[24]

Kinetic Studies of MB Adsorption Using VCIH and CIH Figure 4 shows the effect of contact time on the adsorption of MB onto VCIH and CIH1000. The amount of MB adsorbed increased with increasing adsorption temperature. Adsorption equilibrium was reached at ~24 h under our experimental conditions. Various chemical and/or physical parameters were controlled to manipulate the adsorption kinetics to facilitate the adsorption process.[24] To elucidate the adsorption mechanism and sorption kinetics of MB onto VCIH and CIH1000 under different experimental conditions, two models—specifically, the-pseudo-first-order model (PFOM) and pseudo-second-order model (PSOM)—were used to explore the relationship between the adsorption capacity and contact time.[22]

The PFOM is given as[25]

$$\ln(q_e - q_t) = \ln q_e - k_1 t, \quad (3)$$

where q_e (mg/g) is the adsorption capacity of MB at equilibrium, q_t (mg/g) is the adsorption capacity of MB at time t, and k_1 (1/h) is the overall constant in the PFOM.

The PSOM is given as[26]

$$\frac{t}{q_t} = \frac{t}{q_e} + \frac{1}{k_2 \times q_e^2}, \quad (4)$$

where k_2 (g/mg/h) is the pseudo-second-order adsorption constant.

Table 3 represents the results of kinetic data fit using the PFOM and the PSOM. In the PSOM, the value of the correlation coefficient ($0.989 \leq r \leq 0.997$) is high. The value of $q_{e,cal}$ was closer to the value of $q_{e,exp}$ in the PSOM. Therefore, the PSOM is more feasible for describing the process of MB adsorption onto VCIH and CIH1000, which indicates that chemisorption was the rate-limiting step in the adsorption process.[27] Previous investigations have reported that the chemical adsorption process involves valence forces exerted through the sharing or exchange of electrons between the adsorbate and adsorbent.[28-30]

Effect of pH on the Adsorption of MB onto VCIH and CIH1000 Adsorption is strongly influenced by solution pH, which plays a critical role in the process of adsorbing adsorbates from aqueous media.[11] The MB adsorption ability of VCIH and CIH1000 under different pH conditions is shown in Fig. 5. The amount of MB adsorbed onto VCIH increased with increasing solution pH. Conversely, the amount of MB adsorbed onto CIH1000 did not change with increasing/decreasing solution pH. When VCIH is used, MB, a cationic dye, acquires a positive charge in solution and its adsorption is favored by basic pH conditions. The increase in hydroxide ion concentration accompanying an increase in solution pH creates a negative charge on the adsorbent.[11] In addition, the pH_{pzc} of VCIH was found to be 4.26. Therefore, the electrostatic attraction between VCIH and negative adsorption sites improves its adsorption ability. Similar trends have been observed in previous studies.[31-33] Also, in the case of

Table 2. Langmuir and Freundlich Constants for the Adsorption of MB

Samples	Temp. (°C)	Freundlich constants			Langmuir constants		
		log$k$	1/n	r	Ws (mg/g)	α	r
VCIH	7	0.69	0.13	0.895	10.4	0.19	0.921
	25	0.52	0.31	0.803	17.6	0.15	0.997
	45	1.10	0.13	0.847	25.6	0.47	0.994
CIH1000	7	1.35	0.44	0.944	292.2	0.06	0.990
	25	1.94	0.26	0.948	381.3	5.50	0.990
	45	1.94	0.31	0.963	451.2	2.45	0.915

Table 3. Fitting Results of Kinetic Data Using Pseudo-First-Order Model and Pseudo-Second-Order Model

Adsorbent	$q_{e,exp}$ (mg/g)	Pseudo-first-order model			Pseudo-second-order model		
		k_1 (1/hr)	$q_{e,cal}$ (mg/g)	r	k_2 (g/mg/hr)	$q_{e,cal}$ (mg/g)	r
VCIH	17.1	0.099	8.12	0.957	0.038	17.25	0.997
CIH1000	385.2	0.110	256.3	0.945	0.0009	401.6	0.989

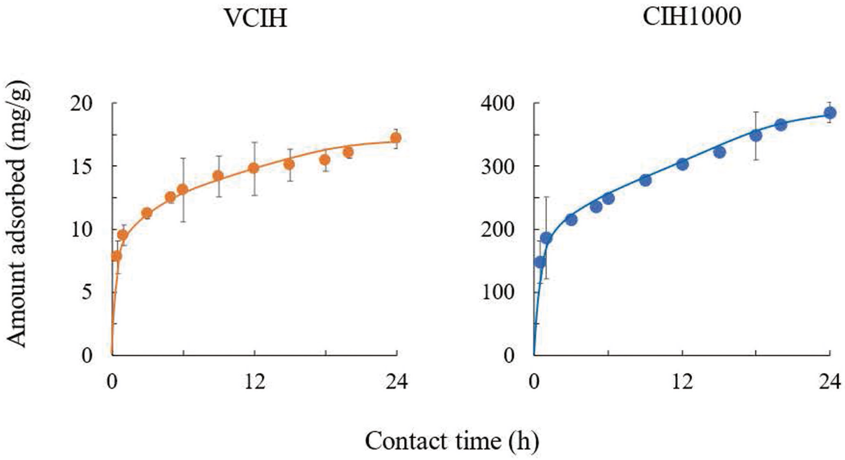

Fig. 4. Effect of Contact Time on the Adsorption of MB onto VCIH or CIH1000

Initial concentration: 1000 mg/L, sample volume: 50 mL, adsorbent: 0.05 g, temperature: 25°C, contact time: 30 min, 1, 3, 5, 6, 9, 12, 15, 18, 20, and 24 h, 100 rpm

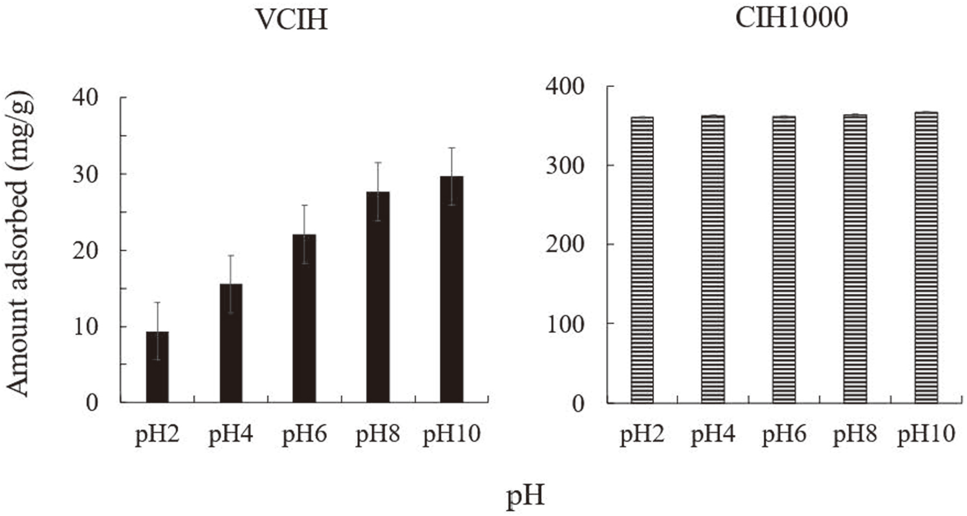

Fig. 5. Effect of pH on the Adsorption of MB onto VCIH or CIH1000

Initial concentration: 1000 mg/L, sample volume: 50 mL, adsorbent: 0.05 g, temperature: 25°C, pH: 2, 4, 6, 8, and 10, contact time: 24 h, 100 rpm

CIH1000, our results indicate that the adsorption capacity is less sensitive to variations in the initial pH of the MB solution. The amount of MB adsorbed remained almost constant over the pH range 2–10. The authors of previous studies have reported that excess hydrogen ion and/or hydroxide ion in the solution strongly affects the MB adsorption capacity.[34] In addition, other mechanisms such as π–π electron donor–acceptor interactions or pore-filling mechanisms might prove beneficial for adsorption.[35]

Mechanism of MB Adsorption onto VCIH and CIH1000 In the preceding sections, we evaluated the adsorption mechanism of MB by demonstrating the effects of initial concentration, temperature, contact time, and pH on its adsorption. To elucidate the adsorption mechanism of MB in detail, we characterized the elemental distribution (carbon, nitrogen, and sulfur, which are components of MB) and binding energies (Figs. 6 and 7, respectively). The values of each element intensity significantly and/or slightly increased after the adsorption of MB. In addition, the carbon energy (285 eV) was detected and found to substantially increase. By contrast, no changes were observed in the sulfur energy (165 and 225 eV) and nitrogen energy (398 eV). Finally, the MB adsorption capacities of VCIH and CIH1000 were compared with those of other reported adsorbents (Table 4).[34, 36-38] CIH1000 adsorbed MB more efficiently than the other adsorbents except SCG-K and SCG-KU. These results indicate that the prepared CIH1000 is a promising adsorbent for removing MB from aqueous media.

In conclusion, this study showed that CIH1000 exhibits good ability to adsorb MB from aqueous media and can potentially contribute to the purification of wastewater containing MB. In addition, the elemental distribution and binding energies of MB were characterized to elucidate its adsorption mechanism. Our findings provide a new perspective on the adsorption of MB and introduce a promising adsorbent for the removal of MB from wastewater.

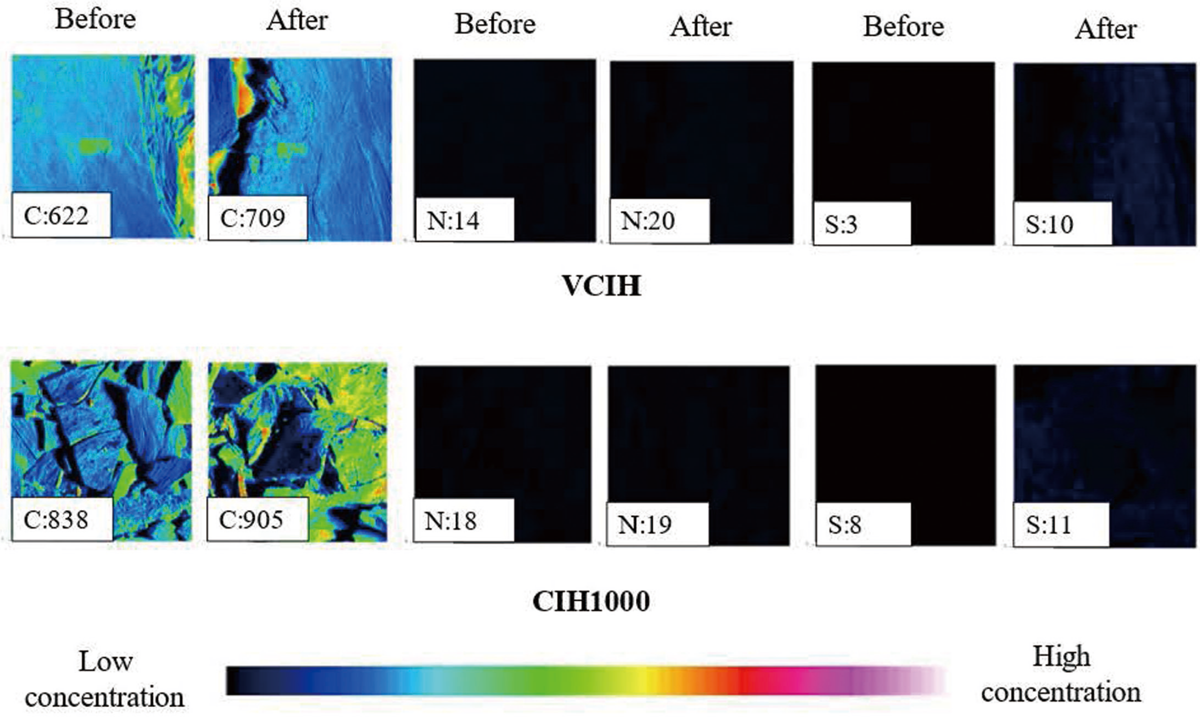

Fig. 6. Qualitative Analysis of Adsorbent Surface before and after Adsorption

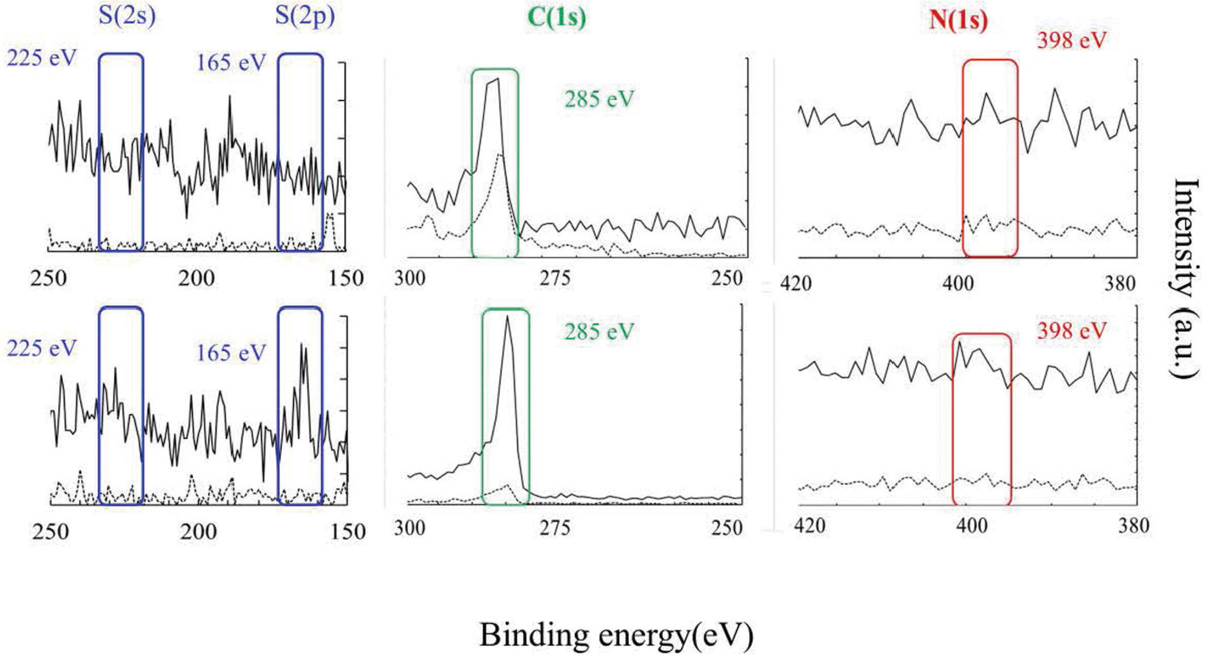

Fig. 7. Binding Energy of Adsorbent Surface before and after Adsorption

Table 4. Comparison of MB Adsorption Capacity with Other Reported Adsorbents

Samples	Adsorption capability (mg/g)	pH	Temp. (°C)	Initial concentration (mg/L)	Contact time (h)	Adsorbent (g/L)	References
SACH AC	88.1	8.0	30	500	1	5	Deivasigamani *et al*., 2023
Activated coffee husk	357.38	7	30	50-500	16	1	Hien Tran *et al*., 2021
Activated coffee husk	316.46	7	30	50-500	16	1	Hien Tran *et al*., 2021
Fe_3O_4-CHBNC	51.02	7.5	25-45	20	4	5	Kochito *et al*., 2023
Fe_3O_4-KLBNC	78.13	7.5	25-45	20	4	5	Kochito *et al*., 2023
SCG-K	389.20	10	20	200	3.3	0.3	Sukhbaatar *et al*., 2021
SCG-KU	499.90	6	50	200	3.3	0.3	Sukhbaatar *et al*., 2021
CIH1000	381.3	-	25	1000	24	1	This study

Acknowledgments This research was supported in part by JSPS KAKENHI Grant Number JP22K06674.

Conflict of interest The authors declare no conflict of interest.

REFERENCES

1) Hazzaa R, Hussein M. Adsorption of cationic dye from aqueous solution onto activated carbon prepared from olive stones. *Environ. Technol. Innov.*, **4**, 36–51 (2015).
2) Shanmugam BK, Easwaran SN, Mohanakrishnan AS, Kalyanaraman C, Mahadevan S. Biodegradation of tannery dye effluent using Fenton's reagent and bacterial consortium: A biocalorimetric investigation. *J. Environ. Manage.*, **242**, 106–113 (2019).
3) Gupta VK, Jain R, Nayak A, Agarwal S, Shrivastava M. Removal of the hazardous dye—tartrazine by photodegradation on titanium dioxide surface. *Mater. Sci. Eng. C*, **31**, 1062–1067 (2011).
4) Katheresan V, Kansedo J, Lau SY. Efficiency of various recent wastewater dye removal methods: a review. *J. Environ. Chem. Eng.*, **6**, 4676–4697 (2018).
5) Jawad AH, Rashid RA, Ishak MAM, Wilson LD. Adsorption of methylene blue onto activated carbon developed from biomass waste by H_2SO_4 activation: kinetic, equilibrium and thermodynamic studies. *Desalination Water Treat.*, **57**, 25194–25206 (2016).
6) Tan IAW, Hameed BH, Ahmad AL. Equilibrium and kinetic studies on basic dye adsorption by oil palm fibre activated carbon. *Chem. Eng. J.*, **127**, 111–119 (2007).
7) Foo KY, Hameed BH. Preparation, characterization and evaluation of adsorptive properties of orange peel based activated carbon via microwave induced K_2CO_3 activation. *Bioresour. Technol.*, **104**, 679–686 (2012).
8) Hameed BH. Spent tea leaves: a new non-conventional and low-cost adsorbent for removal of basic dye from aqueous solutions. *J. Hazard. Mater.*, **161**, 753–759 (2009).
9) Pathania D, Sharma S, Singh P. Removal of methylene blue by adsorption onto activated carbon developed from Ficus carica bast. *Arab. J. Chem.*, **10**, S1445–S1451 (2017).
10) Tran TH, Le AH, Pham TH, Nguyen DT, Chang SW, Chung WJ, Nguyen DD. Adsorption isotherms and kinetic modeling of methylene blue dye onto a carbonaceous hydrochar adsorbent derived from coffee husk waste. *Sci. Total Environ.*, **725**, 138325 (2020).
11) Krishna Murthy TP, Gowrishankar BS, Hari Krishna R, Chandraprabha MN, Baby Mathew B. Magnetic modification of coffee husk hydrochar for adsorptive removal of methylene blue: Isotherms, kinetics and thermodynamic studies. *Environ. Chem. Ecotoxi*, **2**, 205–212 (2020).
12) Murthy TPK, Gowrishankar BS, Chandra Prabha MN, Kruthi M, Hari Krishna R. Studies on batch adsorptive removal of malachite green from synthetic wastewater using acid treated coffee husk: equilibrium, kinetics and thermodynamic studies. *Microchem. J.*, **146**, 192–201 (2019).
13) Pietrzyk P, Borowska EI, Hejduk P, Camargo BC, Warczak M, Nguyen TP, Pregowska A, Gniadek M, Szczytko J, Wilczewski S, Osial M. Green composites based on volcanic red algae Cyanidiales, cellulose, and coffee waste biomass modified with magnetic nanoparticles for the removal of methylene blue. *Environ. Sci. Pollut. Res. Int.*, **30**, 62689–62703 (2023).
14) Ma H, Feng L, Kang M, Yang Z, Zhang R, Li H, Lü C. Potential low-cost biosorbent modified from yard waste for acid-fuchsin removal. *J. Environ. Eng.*, **146**, (2020).
15) Faria PCC, Orfão JJM, Pereira MFR. Adsorption of anionic and cationic dyes on activated carbons with different surface chemistries. *Water Res.*, **38**, 2043–2052 (2004).
16) Lee G, Chen C, Yang ST, Ahn WS. Enhanced adsorptive removal of fluoride using mesoporous alumina. *Microporous Mesoporous Mater.*, **127**, 152–156 (2010).
17) Yokoyama R, Hayashi S, Nakanishi M, Takada J. NO_3-N adsorption property of Ca-containing charcoal. *Mizu Kankyo Gakkaishi*, **31**, 47–52 (2008).
18) Al-Ghouti MA, Al-Absi RS. Mechanistic understanding of the adsorption and thermodynamic aspects of cationic methylene blue dye onto cellulosic olive stones biomass from wastewater. *Sci. Rep.*, **10**, 15928 (2020).
19) Silva C, Gama B, Gonçalves A, Medeiros J, Abud A. Basic-dye adsorption in albedo residue: effect of pH, contact time, temperature, dye concentration, biomass dosage, rotation and ionic strength. *J. King Saud Univ. Eng. Sci.*, **32**, 351–359 (2019).
20) Langmuir I. The adsorption of gases on plane surfaces of glass, mica and platinum. *J. Am. Chem. Soc.*, **40**, 1361–1403 (2002).
21) Freundlich H. Über die Adsorption in Lösungen. *Z. Phys. Chem.*, **57U**, 385–470 (1907).
22) Tang Y, Alam MS, Konhauser KO, Alessi DS, Xu S, Tian W. Influence of pyrolysis temperature on production of digested sludge biochar and its application for ammonium removal from municipal wastewater. *J. Clean. Prod.*, **209**, 927–936 (2019).
23) Yang X, Wang Z, Jing M, Liu R, Jin L, Shen X. Efficient removal of dyes from aqueous solution by mesoporous nanocomposite Al_2O_3/$Ni_{0\cdot 5}Zn_{0\cdot 5}Fe_2O_4$ microfibers. *Water Air Soil Pollut.*, **225**, 1–12 (2014).
24) Cao JS, Lin JX, Fang F, Zhang MT, Hu ZR. A new absorbent by modifying walnut shell for the removal of anionic dye: kinetic and thermodynamic studies. *Bioresour. Technol.*, **163**, 199–205 (2014).
25) Lagergren S. Zur theorie der sogenannten adsorption geloster stoffe. Kungliga svenska vetenskapsakademiens. *Handlingar*, **24**, 1–39 (1898).
26) Ho YS, McKay G. Sorption of dye from aqueous solution by peat. *Chem. Eng. J.*, **70**, 115–124 (1998).
27) Zhou Y, Fu S, Zhang L, Zhan H, Levit MV. Use of carboxylated cellulose nanofibrils-filled magnetic chitosan hydrogel beads as adsorbents for Pb(II). *Carbohydr. Polym.*, **101**, 75–82 (2014).
28) Dawood S, Sen TK. Removal of anionic dye Congo red from aqueous solution by raw pine and acid-treated pine cone powder as adsorbent: equilibrium, thermodynamic, kinetics, mechanism and process design. *Water Res.*, **46**, 1933–1946 (2012).
29) Ma H, Li JB, Liu WW, Miao M, Cheng BJ, Zhu SW. Novel synthesis of a versatile magnetic adsorbent derived from corncob for dye removal. *Bioresour. Technol.*, **190**, 13–20 (2015).
30) Wang Z, Xiang B, Cheng R, Li Y. Behaviors and mechanism of acid dyes sorption onto diethylenetriamine-modified native and enzymatic hydrolysis starch. *J. Hazard. Mater.*, **183**, 224–232 (2010).
31) Murthy TPK, Gowrishankar BS, Chandra Prabha MN, Kruthi M, Hari Krishna R. Studies on batch adsorptive removal of malachite green

from synthetic wastewater using acid treated coffee husk: equilibrium, kinetics and thermodynamic studies. *Microchem. J.*, **146**, 192–201 (2019).

32) Hosseinzadeh H, Ramin S. Fabrication of starch-graft-poly(acrylamide)/graphene oxide/hydroxyapatite nanocomposite hydrogel adsorbent for removal of malachite green dye from aqueous solution. *Int. J. Biol. Macromol.*, **106**, 101–115 (2018).

33) Soleimani H, Mahvi AH, Yaghmaeian K, Abbasnia A, Sharafi K, Alimohammadi M, Zamanzadeh M. Effect of modification by five different acids on pumice stone as natural and low-cost adsorbent for removal of humic acid from aqueous solutions - application of response surface methodology. *J. Mol. Liq.*, **290**, 111181 (2019).

34) Sukhbaatar B, Yoo B, Lim JH. Metal-free high-adsorption-capacity adsorbent derived from spent coffee grounds for methylene blue. *RSC Adv.*, **11**, 5118–5127 (2021).

35) Rafatullah M, Sulaiman O, Hashim R, Ahmad A. Adsorption of methylene blue on low-cost adsorbents: a review. *J. Hazard. Mater.*, **177**, 70–80 (2010).

36) Deivasigamani P, Senthil Kumar P, Sundaraman S, Soosai MR, Renita AA, M K, Bektenov N, Baigenzhenov O, D V, Kumar J A. Deep insights into kinetics, optimization and thermodynamic estimates of methylene blue adsorption from aqueous solution onto coffee husk (Coffee arabica) activated carbon. *Environ. Res.*, **236**, 116735 (2023).

37) HHien Tran T. Huong Le H, Huu Pham T, Thanh Nguye D, Duong La D, Woong Chang S, Moon Lee S, Jin Chun W, Duc Nugyen D. Comparative study on methylene blue adsorption behavior of coffee hisl-derived activated carbon materials prepared using hydrothermal and soaking methods. *J. Environ. Chem. Eng.*, **9**, 105362 (2021).

38) Kochito J, Gure A, Tadesse Beyen T, Emmanuel Femi O. Magnetic iron-oxide coffee husk and khat waste biochar nanocomposites for removal of methylene blue from aqueous solution. *Sep. Sci. Plus*, **7**, 2300246 (2024).